R

R0840090

CENTRAL INSTITUTE OF PHYSICS

*) THE FACTORY OF NUCLEAR DEVICES, BUCHAREST

**) INSTITUTE FOR PHYSICS AND TECHNOLOGY OF RADIATION DEVICES, BUCHAREST

IFTAR - LOP-27-1982 . May

Study of the plasma focus ionic component[1)]

A.BOCANCEA*), N.B.MANDACHE**)
V.I.ZAMBREANU**)

Abstract : Experimental results on the energetic characteristics of the plasma focus ionic component, produced in the IPF 2/20 device are presented. For energies greater than approximate 50 keV the energy distributions of the ions emitted forward are well fitted by the exponential function exp(- E/B), where the medium value of B is 48 keV. Most of the distributions have a maximum in the energy range 25-47 keV.

---

1) To be submitted for publication to Revue Roumaine de Physique.

1. INTRODUCTION

The results presented in this paper come in addition to those presented in the previous works /1,7/.

The measurements of the energetic characteristics of the plasma focus ions emitted forward were carried out on the IPF 2/20 device.The energy in the condenser bank was 10 kJ. and the operating voltage was 16 kV.

2. EXPERIMENTAL SET-UP

The plasma focus ionic component was analyzed using a combined time - of - flight and electrostatic deflection method /1,2/.

The analyzing system (fig. 1a) has a modified system of diaphragms in comparison with that presented in /1,2/. The first diaphragm has a conic profile (skimmer)[3] and was used either at a floating potential or at the analyzing system potential.In both cases there were no evident differences ,as compared to previous results.Work with the first diaphragm at floating potential prevents the occurence of discharges between the central electrode and the first diaphragm,separated at 7.5 cm.

Most experiments were carried out without the electric deflection field,with the 1 mm. high ion detector entrance aperture,placed axially (fig. 1 a,b).

Due to the analyzer system acceptance solid angle, only ions emitted in the plasma focus region by a 0.7 x 1.4 mm^2 surface perpendicular to the device axis can reach the detector.

The axis of the analyzing system coincides with the axis of the plasma focus device,within a precision of 1 mm.

Practically for all discharges ion signals were recorded.This leads to the conclusion that either the hot plasma forms reproductible on the device axis,or the emitting region dimensions are comparable with the hot plasma displacement from the device axis,from one discharge to another.

The energy losses of ions,in the hot plasma and in the working gas (Hydrogen at 1.5 Torr),beeing of only a few keV,they have been neglected /4,5/.

The variation of the secondary emission coefficient of electrons,with the energy of the ions incident on the Venetian blind (fig. 1a) is the only factor which determines the dependence of the ion detector response on incident proton energies.The secondary emission coefficient varies only slightly for energies above 20 keV.It thus rises by only 15 % between 20 and 60 keV /6/.

In the following the recorded ion signals have been taken into account only for energies higher than 20 keV.

3. EXPERIMENTAL RESULTS

Using the analyzing system in the monoenergetic mode (fig. 1c) /1,2/ the total ion emission time /7/ has been determined.Fig. 2 presents a typical proton pulse.The energy of the recorded protons is 80 keV.The medium value of the ion emission time is of appr. 50 ns.This value is in good agreement with the emission time of neutrons produced in the first 2.5 cm. from the central electrode,which has been determined with a collimator and a PM - scintillator assembly.

Using a 140 cm. flight base the ion flight time (hundreds of ns.) is much greater than the ion emission time. Hence the energy distribution of the plasma ions can be determined by means of a time - of - flight separation method.

The protons emitted by the plasma focus reach the ion detector (fig. 1a) as protons and H atoms,because the initial beam attains the charge equilibrium state through atomic processes in the background gas.The charge state of the beam has been determined using a special system of entrance apertures (fig. 1d) for the ion detector.When an electric deflection field is applied only H atoms reach the ion detector through the 4 mm. high axial aperture.Protons with energies in a range determined by the electric deflection field and the position of the 6 mm. high aperture,also reach the detector.A typical signal is presented in fig. 3. The proton peak overlaps the H atoms signal throughout the time range corresponding to the energy range of the recorded protons.

The experimental values of the recorded beam charge state coincide, within 15 %, with the equilibrium fractions.

The results presented below have been obtained with an axial detector entrance aperture, without electric deflection field (fig. 1a,b)

For a limited number of discharges a distinct group of high energy ions has been recorded (fig. 4a). On this oscillogram a distinct 260 keV (200 ns.) ion group can be observed.

Using the relation :

$$N = C \cdot N_{osc} \cdot T^3 \qquad (1)$$

where T is the ion flight time and C is a constant, the ion energy distribution N has been obtained from the amplitude of the signal, which was recorded on the oscilloscope (N_{osc}).

Fig. 4b shows the ion energy distribution obtained from the oscillogram presented in fig. 4a. The marked increase of N while decreasing energy is in accordance with the results presented in /7/. For most discharges the ion signals rise sharply (fig. 5a), at high energies (130 - 260 keV). For only one discharge the signal rise started at 400 keV.

This high energy limit of the ionic component is in agreement with the results described in /8,9/, where the existence of high energy deuteron beams has been brought forward by means of a tritium target. The determinations were performed on the same device.

Althouth for some discharges the recorded signals have one or more maxima, this cannot be interpreted as an energy modulation. The ion signals presented in /7/ are characterized by an artificial energy modulation, which was due to an insufficient screening of the ion detector against electromagnetic noise.

There are two different types of ion energy distributions :

- for 70 % of the discharges the ion distributions have a maximum at low energies, in the range 25 - 47 keV (fig. 5b and 6b);
- for 30 % of the discharges the ion distributions rise monotonically towards low energies till 20 keV, where a slight limiting tendency can be observed, (Fig.4.b)

Some ion energy distributions of the first type have

a structure at low energies (fig. 7b).There is one particular energy distribution,of the second type, which rises sharply at low energies, due to a numerous group of low energy ions, visible on the oscillogram (fig. 8a).

The ion energy distributionswere fitted with the functions: $A E^{-\alpha}$ and $C \exp(-E/B)$, where A and C are constants, α and B are parameters.The ion distributions with a maximum were fitted only for energies greater than that corresponding to the maximum.

We assumed that the independent variable was exactly determined,the whole error of the measurement affecting the dependent variable /10/.Thus the error affecting the distribution is :

$$\sigma_N = N\sqrt{\left(\frac{\sigma_{Nosc}}{N_{osc}}\right)^2 + 9\left(\frac{\sigma_T}{T}\right)^2} \qquad (2)$$

where σ_{Nosc} is the error affecting the signal amplitudes and σ_T is the error affecting the ion flight time.

As due to the variation of the secondary emission coefficient with the ions energy,σ_{Nosc}/N_{osc} is $\pm$ 10 % and the maximum value of σ_T/T is $\pm$ 10 %,the main error affecting the ion energy distribution is due to the finite ion emission time.

With only one exception, the fit of the ion energy distributions with $C \exp(-E/B)$ was characterized by a better correlation coefficient /10/ than that with $A E^{-\alpha}$.

The values of B are in the range 20 - 80 keV ,the medium value being $\bar{B}$ = 48 keV.The values for α are whithin the range 1 - 3.3,while the medium value is $\bar{\alpha}$ = 1.8.

Supposing the energy distributions of deuterons are similar to those of protons,on figs. 4b - 8b the $N\cdot\sigma$ curves are also presented.The energies corresponding to the maximum values of $N\cdot\sigma$ are within the range 56 - 106 keV.(σ is the cross section of the D-D fusion reaction). This result is in good agreement with the end - on neutron spectroscopy measurements, performed on the same device.Considering a beam - target mechanism, an axial beam of deuterons,

emitted forward with energies in the range 50 - 80 keV can accont for these measurements.

4. CONCLUSIONS

The maxima of the ion energy distributions, brought forward at low ion energies, cannot be explained by the decrease of the secondary emission coefficient with decreasing ion energy.For instance, in the case of the ion energy distribution presented in fig. 6b,the difference between N at 20 keV and N at 38 keV (corresponding to the maximum) is greater than 20 %, while the secondary emision coefficient varies with only 15 % over a larger energy range (20 - 60 keV) /8/.

The value of the parameter $\bar{E}$ = 48 keV is consistent with that given in /11/.It has to be noticed that the results presented in /11/ were obtained without differential pumping and the fit with exp(-E/50) is valid for energies greater than 150 keV.

The value $\bar{\alpha}$ = 1.8 has to be compared with α =3.5 obtained on a single discharge by /12/.

Acknowledgements

The authors wish to thank the members of the plasma focus group for many discussions and useful suggestions.

REFERENCES

/1/ Cebanu,A.,et al.,Nucl.Fus.Suppl.,Vol. II,p.197 (1981)
/2/ Bocancea,A.,Mandache,N.B.,to be published in Rev.Roum. Phys.(1982)
/3/ Bertalot,L.,et al.,Nucl. Fus. Suppl.,Vol. II,p.177 (1981)
/4/ Barnett,C.F.,et al., Report ORNL - 5206,Vol. I,(1977)
/5/ Mandache,N.B.,Thesis,Univ. of Bucharest,(1980)
/6/ Chambers,E.,Phys. Rev.,133A, 1202,(1964)
/7/ Bocancea,A.,et al., I-th Europ. Conf. on Contr. Fus. and Pl. Phys., Vol. I, D4,Moscow, Sept. (1981)
/8/ Tsois,N.,et al., IEEE Int. Conf. on Pl. Sci., Santa-Fe' 18 - 20 may (1981)
/9/ Tsois,N., Thesis, Central Inst. of Phys., Bucharest(1981)
/10/Bevington,P., "Data Reduction and Error Analysis for the Physical Sciences", Mc Graw - Hill Book Co. (1969)

/11/ Krompholz, L., et al, Appl.Phys., 13, 29 (1977)

/12/ Gerdin, G., et al., J.Appl.Phys., 52, 5, May (1981)

FIGURE CAPTIONS

Fig.1.a. - The ion analyzer system
1. plasma focus electrodes
2. conic diaphragm (skimmer)
3. ceramic tube
4. diaphragm system
5. drift tube
6. electrostatic analyzer entrance aperture
7. deflection plates
8. electrostatic analyzer exit aperture (ion detector entrance aperture)
9. Venetian-blind
10. scintillator
11 photomultiplier

Fig.1.b. - Axial aperture

Fig.1.c. - Aperture for monoenergetic determinations

Fig.1.d. - Aperture system for ionic component charge state determinations

Fig.2. - Typical oscillogram of 80 keV proton pulse

Fig.3. - Typical oscillogram in the case of ion beam charge state determinations

Fig.4.a. - Analyzer system output signal

Fig.4.b. - Ion energy distribution ; $N\sigma$ function

Fig.5.a. - Analyzer system output signal

Fig.5.b. - Ion energy distribution ; $N\sigma$ function ;
Dotted line - the function $\exp(-R/60)$

Fig.6.a. - Analyzer system output signal

Fig.6.b. - Ion energy distribution ; $N\sigma$ function ;
Dotted line - the function $\exp(-R/21)$

Fig.7.a. - Analyzer system output signal ;

Fig.7.b. - Ion energy distribution ; $N\sigma$ function

Fig.8.a. - Analyzer system output signal

Fig.8.b. - Ion energy distribution ; $N\sigma$ function

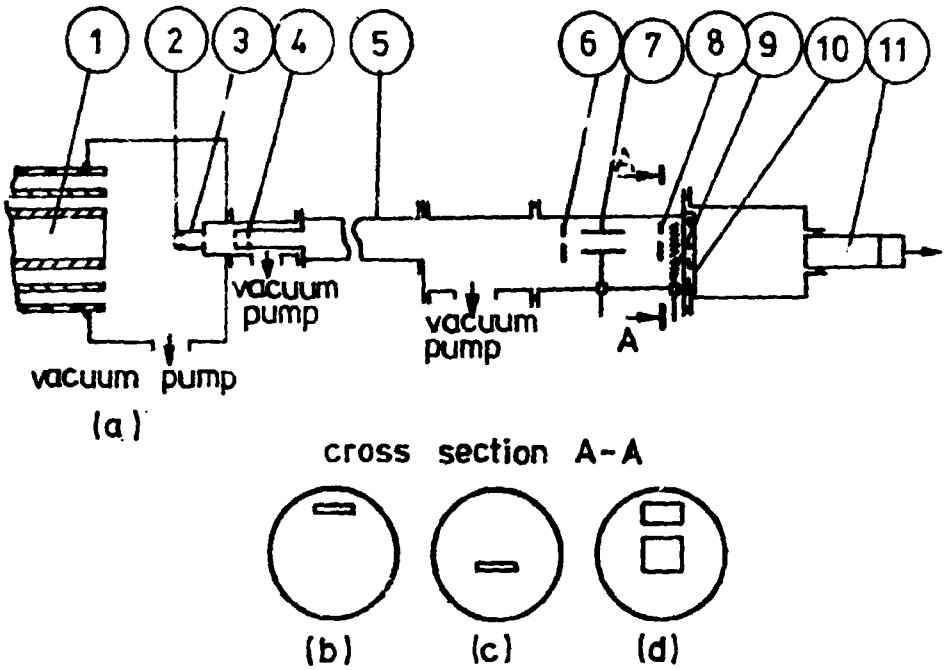

FIG.1

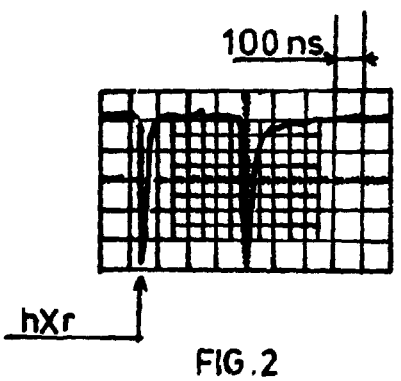

FIG.2

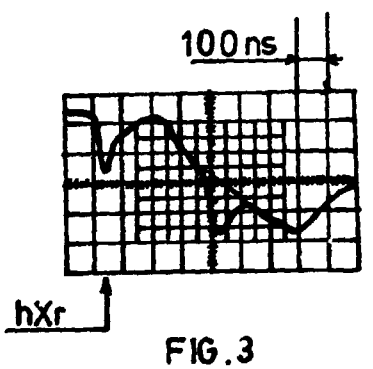

FIG.3

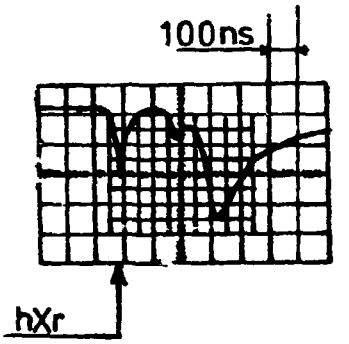
100ns
hXr

FIG. 4a

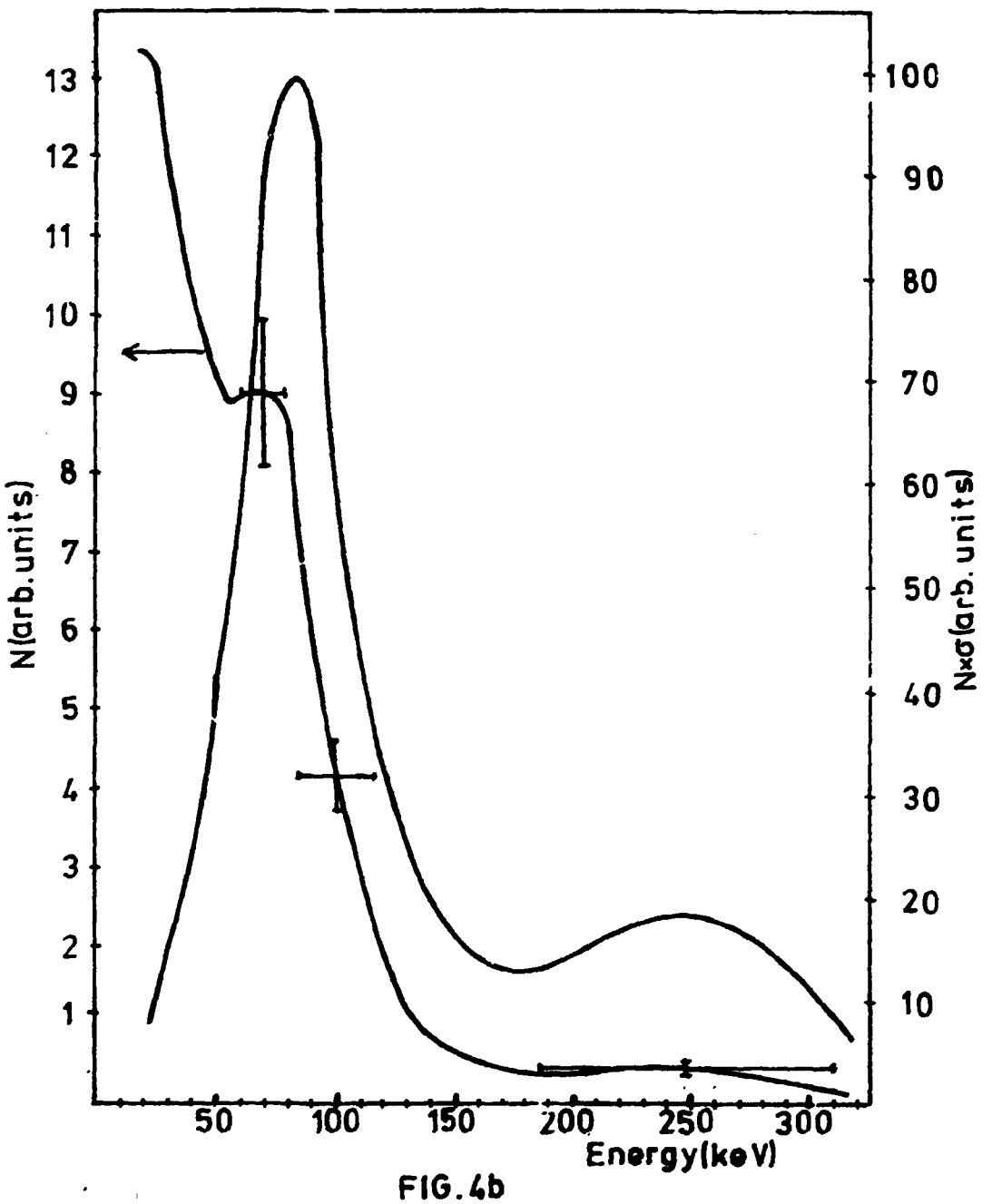
N(arb.units)
Nxσ(arb.units)
Energy(keV)
13
12
11
10
9
8
7
6
5
4
3
2
1
100
90
80
70
60
50
40
30
20
10
50
100
150
200
250
300

FIG. 4b

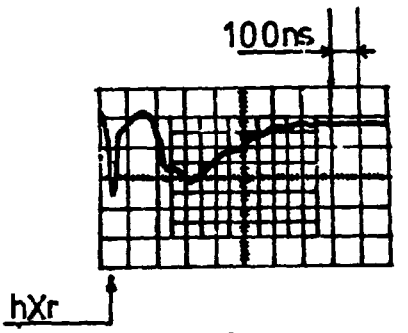
100ns
hXr

FIG. 5a

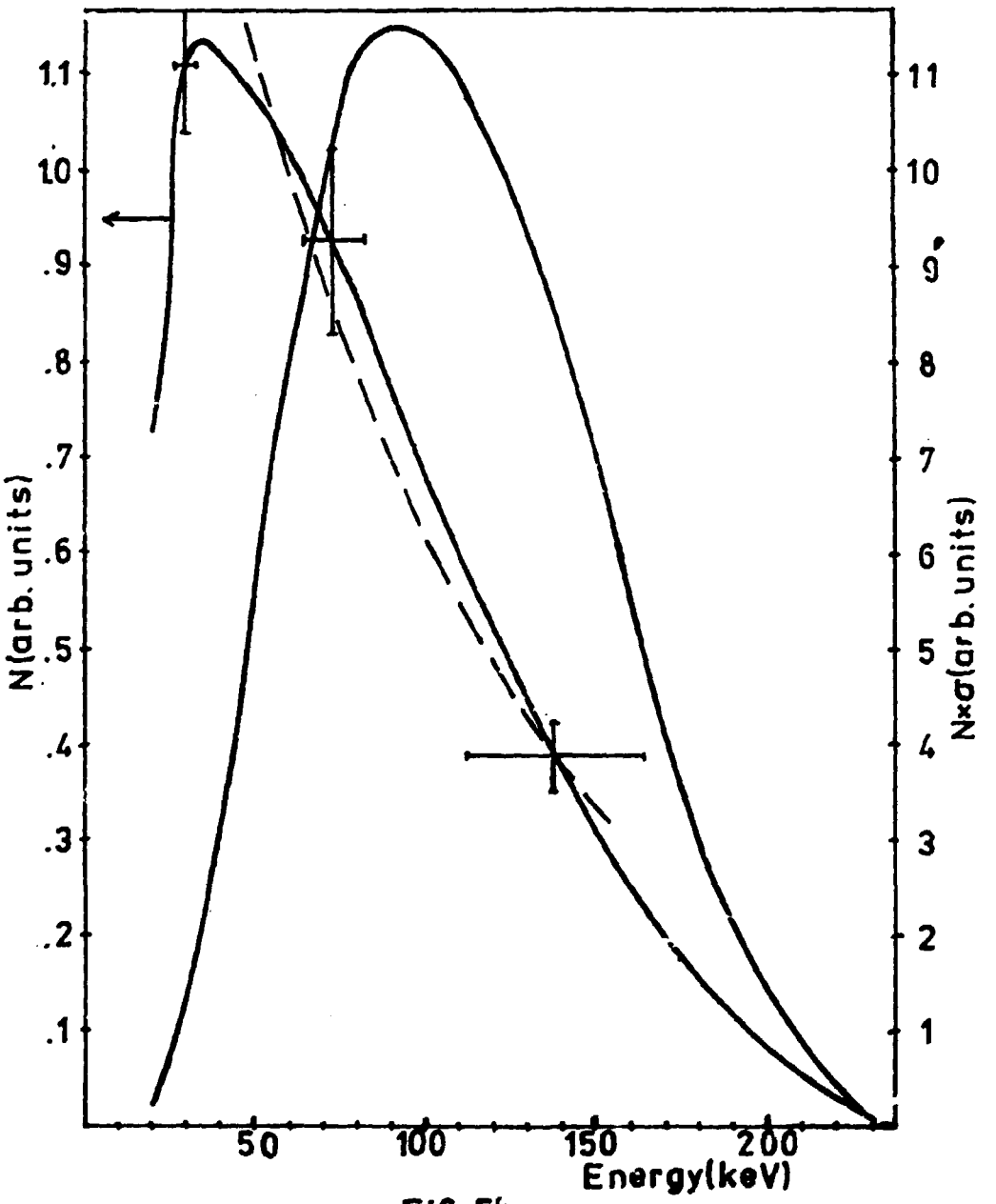
N(arb. units)
Nxσ(arb. units)
Energy(keV)
1.1
1.0
.9
.8
.7
.6
.5
.4
.3
.2
.1
11
10
9
8
7
6
5
4
3
2
1
50
100
150
200

FIG. 5b

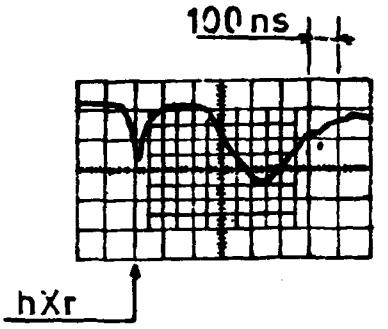
100 ns
hXr

FIG.6a

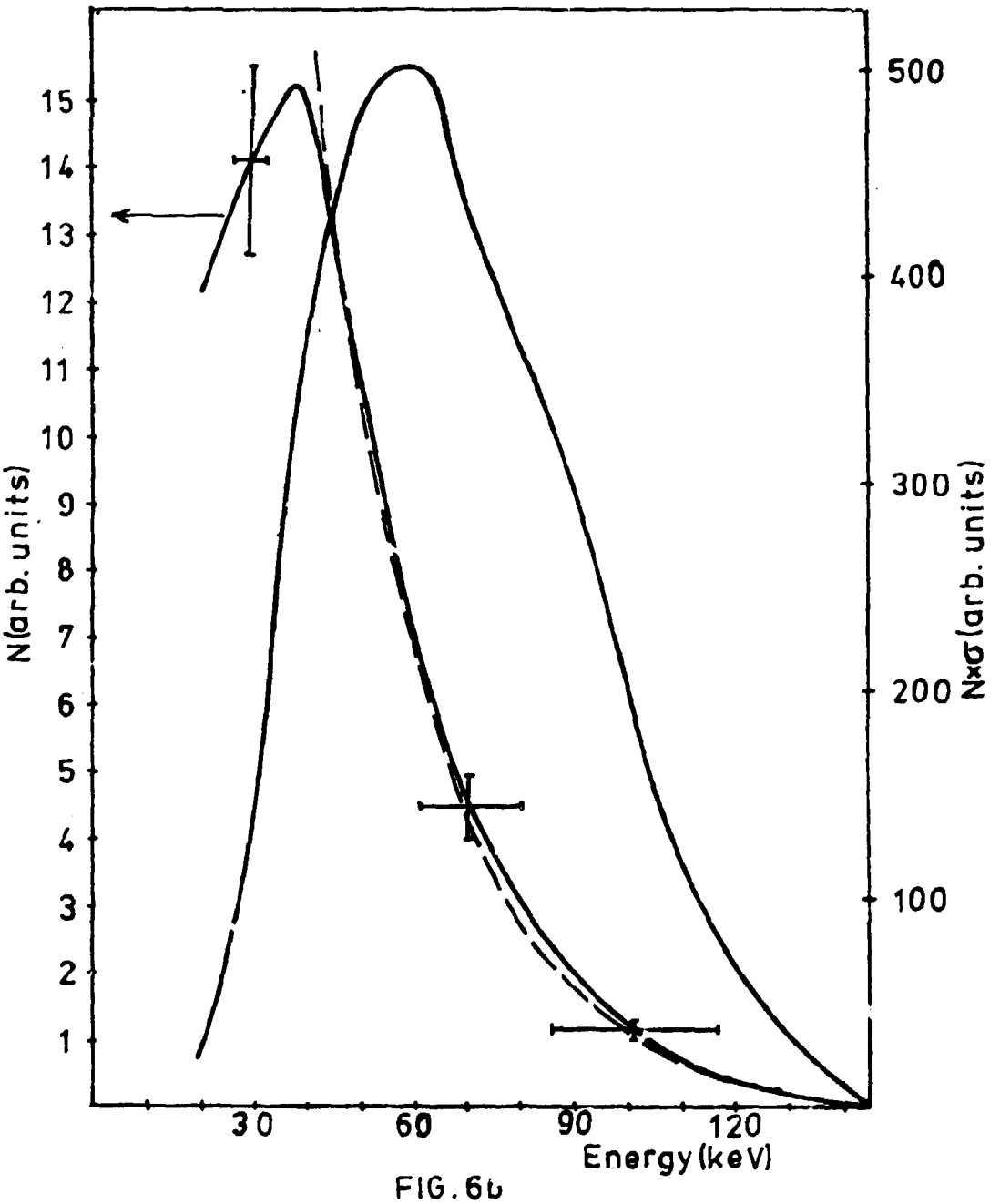
N(arb. units)
Nxσ(arb. units)
Energy (keV)
30
60
90
120
1
2
3
4
5
6
7
8
9
10
11
12
13
14
15
100
200
300
400
500

FIG.6b

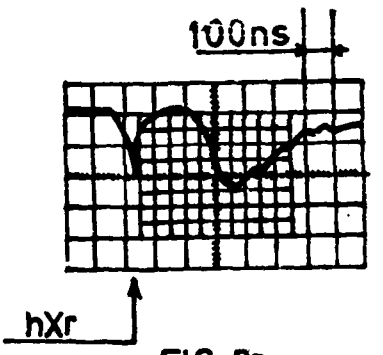
100ns
hXr

FIG.7a

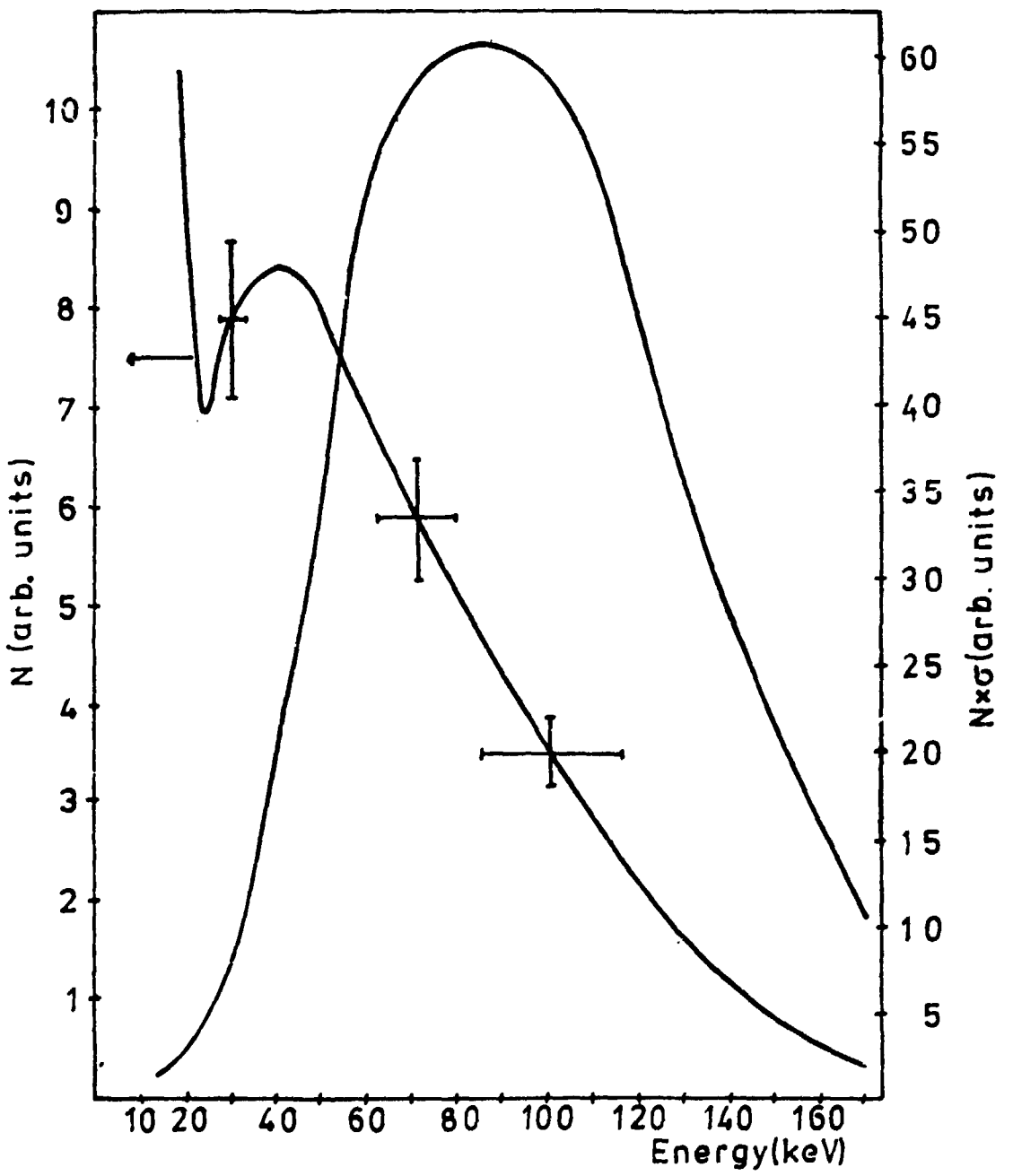
N (arb. units)
Nxσ(arb. units)
Energy(keV)
10 20 40 60 80 100 120 140 160
1 2 3 4 5 6 7 8 9 10
5 10 15 20 25 30 35 40 45 50 55 60

FIG.7b

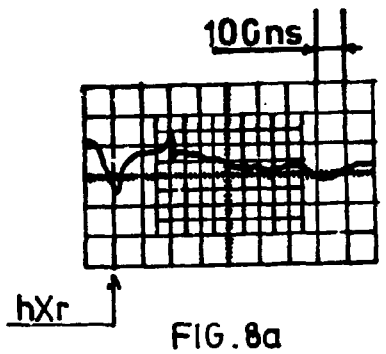
100ns
hXr

FIG.8a

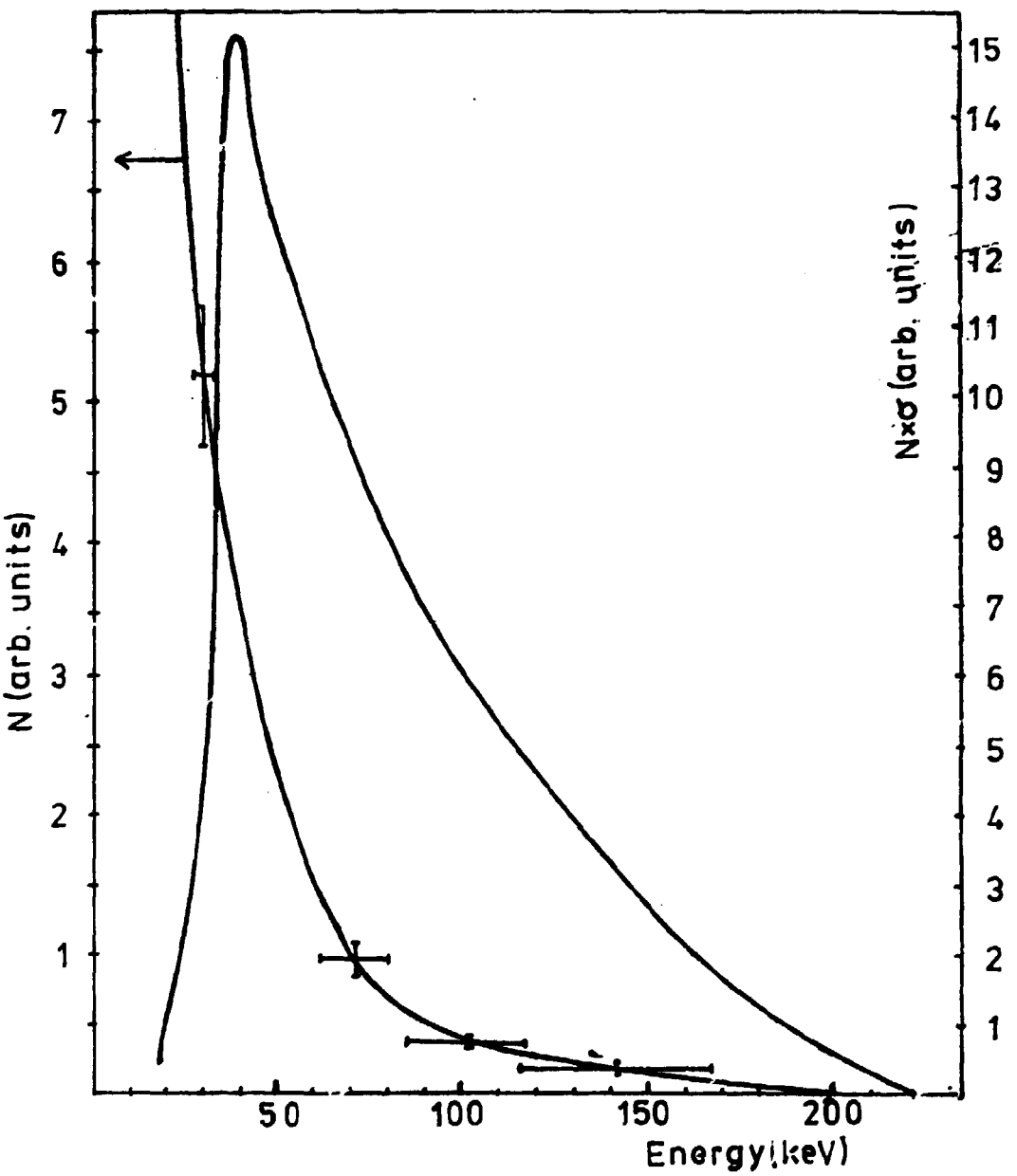
N (arb. units)
Nxσ (arb. units)
Energy(keV)
50
100
150
200
1
2
3
4
5
6
7
8
9
10
11
12
13
14
15

FIG.8b